Curvature generation based on weight-updated boosting using shoe last point-cloud measurements

Wang, D., Li, Z., Dey, N., Misra, B., Sherratt, R. S. ORCID: https://orcid.org/0000-0001-7899-4445 and Shi, F. (2024) Curvature generation based on weight-updated boosting using shoe last point-cloud measurements. Heliyon, 10 (4). e26498. ISSN 2405-8440 doi: https://doi.org/10.1016/j.heliyon.2024.e26498 Available at https://centaur.reading.ac.uk/115299/

Heliyon 10 (2024) e26498

Contents lists available at ScienceDirect

Heliyon

journal homepage: www.cell.com/heliyon

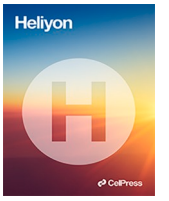

Research article

Curvature generation based on weight-updated boosting using shoe last point-cloud measurements

Dan Wang [a], Zairan Li [a,*], Nilanjan Dey [b], Bitan Misra [b], R. Simon Sherratt [c], Fuqian Shi [d]

[a] Wenzhou Polytechnic, Wenzhou, 325035, PR China
[b] Department of Computer Science and Engineering, Techno International New Town, Kolkata, 700156, India
[c] Department of Biomedical Engineering, The University of Reading, Reading, UK
[d] Rutgers Cancer Institute of New Jersey, New Brunswick, 08903, USA

ARTICLE INFO

Keywords:
Comfort shoes
Ensemble learning
Point-cloud dataset
Shoe last customizing

ABSTRACT

Lasts are foot-shaped forms made of plastic, wood, aluminum, or 3D-printed plastic. The last of a shoe determines not only its shape and style but also how well it fits and protects the foot. A weight-updated boosting-based ensemble learning (WUBEL) algorithm is presented in this paper to extract critical features (points) from plantar pressure imaging to optimize the shoe's last surface to satisfy a comfortable shoe's last surface optimization design. An enhanced last design is constructed from the foot measurement data of the bottom surface of the base last, the critical control lines (points) of the shoe's last body, and the running-in degree of the pressure-sensitive area lattice data. Using a Likert scale (LS) and relevant evaluation indicators, we conducted an experimental evaluation and comparative study of our enhanced last design. With a point-cloud dataset, the proposed method performs highly effectively in constructing shoes, which will help diabetes patients find comfortable and customized shoes.

1. Introduction

Shoes are an essential item in our daily lives, serving not only as a means of protection for our feet but also as an aesthetically pleasing and spiritually fulfilling accessory. With the rise in living standards, people's expectations for footwear have also increased, demanding not only comfort but also style, color, and fashion. To achieve comfortable footwear, the shoe last design plays a crucial role. It is necessary to ensure that the shoe is comfortable before it is finished. Plantar pressure analysis is commonly used to optimize shoe last design by creating a point cloud measurement dataset through human pressure measurement data [1,2]. The objectives of the research are to develop a robust algorithm for processing point-cloud measurements of shoe lasts and generating accurate curvature profiles and to improve comfort and fit for shoe wearers. Deep learning (DL), a mainstay of artificial intelligence (AI), has successfully addressed various two-dimensional vision problems [3,4]. However, point cloud data differ from image data, as they do not encode spatial relationships between pixels. Thus, deep learning models for image recognition require additional processing for point cloud data. Methods such as reordering disordered data, performing data augmentation with all permutations, using recurrent neural networks (RNNs), and using asymmetric functions ensure permutation invariance when processing point cloud data [5,6]. Additionally, invariance should also apply to rotation and translation. Therefore, aligning the input point cloud, altering the pose, using shared

* Corresponding author.
E-mail address: lzr198206@126.com (Z. Li).

https://doi.org/10.1016/j.heliyon.2024.e26498
Received 22 May 2023; Received in revised form 12 February 2024; Accepted 14 February 2024
Available online 20 February 2024

weights in convolution, and utilizing farthest point sampling (FPS) and hierarchical feature extraction are necessary when using point cloud data for deep learning. In conclusion, optimizing shoe last design is critical in achieving comfortable and fashionable footwear. The use of plantar pressure analysis and DL methods on point cloud datasets can greatly improve the design process. However, additional processing is necessary to ensure permutation and spatial invariance, which can be achieved through various techniques, such as reordering, data augmentation, and pose alignment. With continued research and development, we can expect even more advanced techniques to further enhance the design and manufacturing of comfortable and stylish footwear [7,8].

Among all deep learning technologies currently, ensemble learning (EL) is one of the most powerful deep learning technologies available that combines several weak learners to overcome the shortcomings listed above. An ensemble learning indicator is usually a decision tree. In most cases, a decision tree is used as an indicator of ensemble learning. Various components of the eigenvector are then compared to the threshold of the decision tree node to determine whether they should be entered into the left or right child node. For classification problems and regression problems, the prediction result is stored in the leaf node as the category value or regression value. Classification regression trees are mostly used to accomplish ensemble learning [9–11]. Classification trees map a multidimensional space with a piecewise linear division, that is, they divide it along a line parallel to each axis; regression trees map a piecewise constant function. Any function on the closed interval can be approximated to any specified accuracy when the interval is finely defined. Therefore, decision trees are suitable for all types of data [12].

In traditional machine learning, several different possible functions are constructed, and a classifier closest to the actual classification function is selected. Decision trees, artificial neural networks, and naive Bayes classifiers are among the most common single classifier models. When classifying new instances, ensemble learning integrates several single classifiers and determines the final classification by combining the classifications of multiple classifiers, resulting in a more accurate classification than a single classifier alone. Compared to a single classifier, the ensemble learning method is equivalent to multiple classifiers deciding together. A single ensemble classifier can be an artificial neural network classifier. As a final classification, the combined output of the integrated classifier is obtained from the output of each artificial neural network based on the same input [13]. Integrating the basic classifiers based on different feature sets and studying methods such as linear integration, winner-take-all (WTA), and evidence reasoning is a promising research direction. As a result of linear integration, the outputs of each basic classifier are combined linearly as the classification results. Zhao et al. [14] developed multiview-based random rotation ensemble pruning (MVRR-EP) as a technique for improving weak classifiers to strong ones. Ma et al. [15] developed ensemble learning using multiple features and performed a visual inspection system to demonstrate the advanced and practical nature of the proposed algorithm.

Based on approximate probability theory, strongly learnable objects are those that can be learned with high accuracy by a polynomial learning algorithm. A weakly learnable system is slightly more accurate than random guessing. Strongly learnable objects must be weakly learnable as a sufficient condition. Algorithms that are weakly learnable are generally easier to obtain than algorithms that are strongly learnable. This means that the best method of improving the learning algorithm is to start with a weak learning algorithm, obtain many weak classifiers, and combine the weak classifiers to form a strong learning algorithm. Bagging, also known as bootstrap aggregation, is an ensemble technique that reselects new datasets from the original dataset by sampling with replacement to train the classifier. Using the set of trained classifiers to classify new samples, it counts the classification results of all classifiers by majority vote or averaging the output, and the final label is the one that scored the highest. These algorithms are effective in reducing bias and variance [16]. As an example, 70% of the data from the original data can be set in each round, extract multiple rounds, trained in different classifiers (if the same model is used, the difference will be the parameters), and the test set data can be predicted with k models. The prediction result is determined by using the classifiers that receive the most votes for classification problems. As a result of regression problems, the mean of the predicted values is used. Basically, the training data are collected randomly by random forests [17,18]. Based on ensemble learning, two classifiers were proposed to classify shoe last curvature using point clouds, therefore improving shoe last customization.

Since point cloud data are discrete, no clear modeling method can be demonstrated to be effective. Using point cloud data, nonuniform rational B-splines (NURBS) can adequately fit irregular surfaces. As part of the research on shoe-last shape, NURBS is also shown to be an effective way of fitting the foot because the wearing comfort of footwear is based on the study of psychological quantity. Establishing a relationship between psychological quantity and point cloud data of shoe-last surfaces is one of the biggest challenges and hot topics in footwear comfort research. Deep learning technologies can bridge this data gap.

2. Methodology

2.1. Weights updated boosting ensemble learning

Weight updated algorithms are widely used in decision-making and prediction. They are also widely used in algorithm design and game theory. The simplest use case is forecasting based on expert advice, where a decision-maker must continually decide on an expert's advice. Initial weights are assigned to experts (usually the same initial weights), and these weights are updated, multiplicatively and iteratively, based on feedback from the expert's performance.

The objective of traditional machine learning algorithms (e.g., decision trees, artificial neural networks, support vector machines, naive Bayes, etc.) is to find an optimal classifier that separates training data as much as possible. Ensemble learning combines multiple classifiers to produce a classifier with better prediction ability. Since several classifiers have a relationship, it is more likely that the Nth classifier will be divided into the N-th classifier. Currently, a classifier has no paired data, and the previously paired data cannot be paired again. Therefore, each weak classifier has its own most concerned point, and each weak classifier only pays attention to a part of the data in the entire dataset, so they must be combined to be effective. Weighted voting must be performed according to the weight of

the weak classifier. The weight is calculated based on the classification error rate of the weak classifier. The higher the weight is, the lower the error rate of the weak classifier.

For training data $X = \{x_i | i \in N\}$ in classifying space Y, the number of classifiers is h, and e is the error for h. The weighted update algorithm for ensemble learning classifiers is described in Algorithm 1. The recognition error rate is less than 1/2; that is, the learning algorithm that is only slightly more accurate than random guessing is called a weak learning algorithm; the recognition accuracy is extremely high and can be applied in polynomial time. It is referred to as a strong learning algorithm. Iteratively using weak learning of the classifier composition, boosting algorithms add its results to a final strong learned classifier. As part of the joining process, different weights are usually applied according to their classification accuracy. Data points previously misclassified are usually reweighted after weak learners are added to make the classification more accurate. Some recent examples are LPBoost, TotalBoost, BrownBoost, MadaBoost, and LogitBoost. In the AnyBoost framework, many boosting methods can be viewed as gradient descent with convex error functions.

By using a special lifting algorithm, this method can transform a weak learning algorithm into a strong one. First, the base learner is trained by the initial training sample set. Second, the weight of the samples misclassified by the base learner is increased so that these samples receive more attention in the next round of training, and the adjusted samples are applied to train the next base learner. These steps are repeated until several learned classifiers are obtained.

Algorithm 1: Weight updated algorithm for classifiers

REQUIRED: training data-X, labels-Y, weights distribution-w
OUTPUT: classifiers h(x)

INITIALIZE: the weights distribution for training data. The same weights are assigned to each training sample by,

$$D_1 = (w_{11}, w_{12}, \cdots, w_{1m})^T$$

TRAIN the classifiers by

$$h_t(x) = \zeta(D, D_t)$$

CALCULATE: classification error

$$e_t = \sum_{i=1}^{m} w_{ti} I(h_t(x_i) = y_i)$$

Where, $I(h_t(x_i) \neq y_i) = \begin{cases} 0 \ \ if\ h_t(x_i) = y_i \\ 1 \ if\ h_t(x_i) \neq y_i \end{cases}$

UPDATE: weights of classifiers

$$D_{t+1} = (w_{t+1,1}, w_{t+1,2}, \cdots, w_{t+1,m})$$

Where, $w_{t+1,i} = \frac{w_{t,i}}{Z_t} \bullet \begin{cases} e^{-\alpha_t} \ \ if\ h_t(x_i) = y_i \\ e^{\alpha_t} \ \ if\ h_t(x_i) \neq y_i \end{cases} = \frac{w_{t,i}}{Z_t} e^{-\alpha_t h_t(x_i) y_i}$, $\alpha_t = \frac{1}{2} \ln(\frac{1}{e_t} - 1)$, Z is a normalized factor.

WEIGHTED AVERAGE: for $t = 1, 2, \cdots, T$

$$f(x) = \frac{1}{T} \sum_{t=1}^{T} \alpha_t h_t(x)$$

CLASSIFICATION:

$$h(x) = sign(f(x)) = sign(\sum_{t=1}^{T} \alpha_t h_t(x))$$

To obtain predicted values for classification problems, weighted voting is used; for regression problems, the weighted average is used. Details can be found in Algorithm 2.

2.2. Point-cloud dataset-based curvature construction and evaluation

2.2.1. Point cloud dataset-based curvature

Data from the last motherboard are acquired to generate the surface of the bottom of the shoe-last. Senior technicians usually complete these experience data during the production of the shoe-last body. First, the model's library imports the digitized model after it is digitized. Second, it is necessary to obtain the plantar pressure image based on the geometry, pixel structure, and texture segmentation results. A lattice dataset includes the area number, location, lattice coordinate vector, etc. In addition, the boundary point set and control point set of the nonuniform rational basis spline (NURBS) surface must be generated, and then the splicing patch can be smoothed. After that, all the bottom surfaces of the last are seamlessly spliced together [19–21]. The last link is to evaluate the generated last bottom surface, design the evaluation index and combine it with the psychological scale method, and interactively design and modify the last bottom surface through the surface generation program and design software until the last bottom surface that meets the requirements is generated.

Algorithm 2: Enhance weak classifiers to strong using weight update algorithm

REQUIRED: DATA, CLASS_LABELS, ITERATION_NUBER
OUTPUT: weak classification-weak_class

```
wc<-weak_class # the information of weak classifiers
m<-num
D<-1/m)    #weights for start
class_estimation<-0 # set initial to 0 for all classifiers
FORiIN ITERATION_NUBER
    bestStump, error, class_estimation<- buildStump (DATA, CLASS_LABELS, D)   # create a decision tree
      alpha <- float (0.5*log((1.0-error)/max(error,1e-16))) # get weight of the classifier
    bestStump['alpha'] <- alpha #record the best decision stump
    weak_class<-weak_class +bestStump
      epsilon <- multiply (-1*alpha*mat (CLASS_LABELS), class_estimation)
       D <- multiply (D, exp(epsilon)) # update
       D <- D/SUM (D)
    class_estimation<- class_estimation+ alpha* class_estimation
    aggErrors<- multiply(sign(class_estimation) !=mat(class_estimation)) #error
    errorRate<-SUM (aggErrors)/m
    IFerrorRate == 0.0 THEN
    BREAK
    ENDIF
ENDFOR
RETURN weak_class
```

Reverse construction of the shoe last based on the point set of the plantar pressure key region is complex reverse engineering. Through the combination of reverse engineering and rapid prototyping technology, the model can be copied quickly, changing the traditional product development design and manufacturing mode. For the reverse construction of the shoe last, the point cloud data can be divided into 6 base surfaces, including the bottom surface, top surface, and 4 sides. Then, it is realized by the smooth surface splicing algorithm of graphics. Here, more attention is given to the generation of the surface of the bottom of the last, and the method based on the base board of the bottom of the last is adopted, which can greatly reduce the complexity of the surface construction. All graphics algorithms are based on NURBS. This chapter mainly uses the bicubic B-spline surface patch to construct the bottom surface of the last. Initially, a baseline is generated from an NURBS curve; the NURBS curve is defined by its order, a set of weighted control points, and a node vector. NURBS curves and surfaces are the generalizations of B-spline curves and Bezier curves and surfaces. The main difference is the weight of the control points; the weight of the control points can make NURBS curves more perfect to fit industrial products.

To generate an NURBS surface, a set of recursive sequence values must be calculated, denoted as $N_{i,\,n}$. The calculation can be done using:

$$N_{i,n} = f_{i,n} N_{i,(n-1)} + g_{(i+1),n} N_{(i+1),(n-1)} \tag{1}$$

where f and g are linear combination factors, calculated by:

$$f_{i,n}(u) = \frac{u - k_i}{k_{i+n} - k_i} \tag{2}$$

$$g_{i,n}(u) = \frac{k_{i+n} - u}{k_{i+n} - k_i} \tag{3}$$

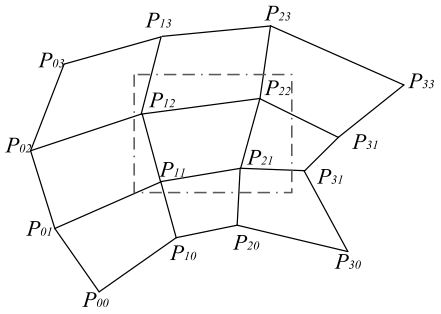

Fig. 1. Bicubic NURS.

where $f_{i,n}(u) + g_{i,n}(u) = 1; k_i$ is the inserted node data. By using Eqns. (1)–(3), the node vector of the NURBS surface is then constructed (bicubic); and let $u = [u_0, u_1, L, u_{m+p}]$, $v = [v_0, v_1, L, v_{n+q}]$, then the $p \times q$ rank NURBS is defined by:

$$p(u,v) = \sum_{i=0}^{m} \sum_{j=0}^{n} P_{i,j} N_{i,p}(u) N_{j,q}(v) \tag{4}$$

where $P_{i,j}$ is a characteristic style called a B-spline surface that constitutes a control network; $N_{i,p}(u)$ and $N_{j,q}(v)$ are NURBS baselines determined by the node vectors U and V according to the deBoor-Cox recursion formula. When $m = n = 3$, it is defined as a bicubic NURBS, as shown in Fig. 1, and the control point of P_{ij} is calculated by Eqn. (4).

Inserting the characteristic data vector of the key area of plantar pressure together with the female last dataset constitutes the NURBS control mesh data of the bottom surface of the last, and the optimal design of the bottom surface of the last is synthesized through the smoothing splicing algorithm presented in the next section. It is preferable to build a NURBS grid line system (Python-NURBS program) through the program and store the node data (the node data will be compared with other key area lattice data later). Fig. 2 shows the NURBS control matrix that determines the position of the curve, usually not on the curve, forming the control polygon. Surface splicing based on the smoothing method is a relatively mature operation at present. So-called smoothing means that the surface is smooth as a whole; mathematically, it can be described as having second-order geometric continuity (G2) or continuity above G3, and there are no inflection point, singular points, or curvature changes uniformly; the control points of the surface change uniformly, with no sudden changes or jumps and no bulges or wrinkles. The G2 continuity is shown in Fig. 3.

In G2, curvature continuity, or radial continuity, two faces/surfaces intersect at the same point, are tangent to each other, and their curvatures are equal along each edge. Therefore, smooth surfaces must have continuous transitions across their edges. In the case of surface reflections, control point stitching is another way to describe the process since it is impossible to tell where one patch ends and another begins. Here, an edge-based splicing method is used for bicubic NURBS surface splicing. When N nonuniform bicubic B-spline surfaces are surrounded by N sides, the nonuniform B-spline surfaces interpolated at the corners are used, and adjacent surfaces only need to have the same corners. The contour deletion mode is unified with the curve subdivision formula interpolated at the corner points. It can be proven that when the outermost two control grids are regular, the first and last edges of each row and column are regular according to the new formula for the nonuniform Catmull-Clark subdivision mode. When the weight of the extended edges is zero, the next layer of control vertices generated by the nonuniform Catmull-Clark subdivision mode is the new control vertex, and the subdivided weights remain in the original control network.

2.2.2. *Curvature evaluation based on running-in degree*

Regarding the effect of the last, it is necessary to exclude the artificial subjective influence in the software design process and only evaluate the impact of the NURBS control points generated by the pressure-sensitive data on the design of the last. There are two kinds of evaluation indicators: one is an evaluation based on the degree of running-in, and the other is based on the psychological scale method. Among them, the second method requires small batch production of shoes and is completed by the wearing comfort evaluation system.

First, the concept of running-in degree is clarified. The running-in degree refers to the comprehensive average value of the distance between the control point set and the point set generated by the intersection of the surface in the z-axis direction. Here, it is necessary to make it clear that the running-in degree can be calculated by the average of the single dimension or the comprehensive average of the three-dimensional space; the distance measure can be customized, such as the Euclidean distance method. Here, a relatively mature method based on NURBS fitting error is used to calculate the degree of running-in, and different datasets are compared, as shown in Fig. 4. The z-axis is a running-in degree based on the example dataset. The x and y here are $u(x)$ and $v(x)$ of the NURBS curvature. We show the running-in degree and NURBS curvature in a 3D-axis system, so the example dataset was reproduced.

Fitting error calculation process: given surface control points $c(i,j)(i = 1,2,\cdots n, j = 1,2,\cdots,m)$ generate node vectors $U = (u_0, u_1, \cdots, u_{n+4})$ and $V = (v_0, v_1, \cdots, v_{m+4})$, the deviation error is:

$$e = \left| q(i,j) - p\left(\widetilde{u}_i, \widetilde{v}_j\right) \right| \tag{5}$$

where $i = 1,2,\cdots,r$, $j = 1,2,\cdots,s$. Accordingly, the degree of running-in can be defined as:

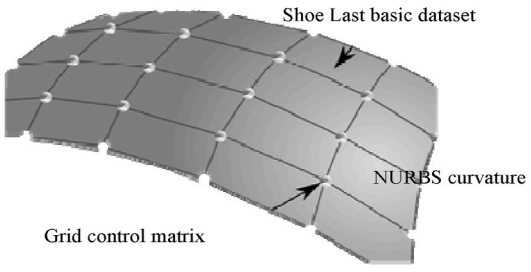

Fig. 2. Shoe last curvature, NURBS and control matrix.

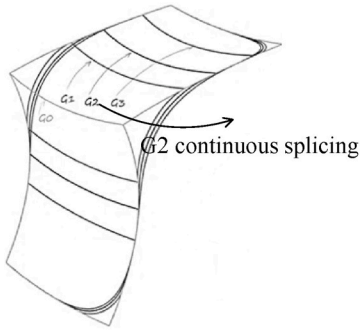

Fig. 3. Smoothing G2 surface stitching.

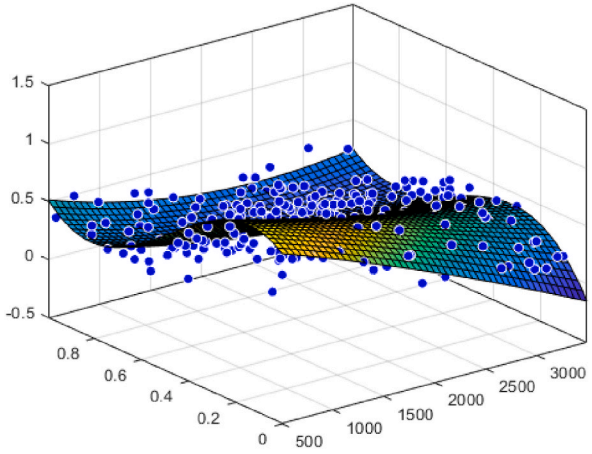

Fig. 4. Calculation of the running-in degree of the relationship between the point set and the surface.

$$\beta = \frac{|e|}{mn\|c\|N_{i,3}(u_i)N_{j,3}(v_j)} \tag{6}$$

where $N(u)$ and $N(v)$ are baselines of NURBS. $\|c\|$ is the vector norm of the control points defined as:

$$\|c\| = |c_i - c_j| = \sum_{k=1}^{l} \sqrt{|c(k,i)^2 - c(k,j)^2|} \tag{7}$$

Fig. 5 shows the pipeline of how the fitting degree of a NURBS is calculated using Eqns. (5)–(7).

3. Results

3.1. Experimental design and measurement data processing

Plantar pressure experiments were conducted using an RSscan foot scanner (RSscan International, Belgium). Sixty healthy volunteers over the age of 18 recruited for the plantar pressure imaging study completed the data collection. In addition to being free of neurological diseases, volunteers were also required to have a normal gait, no walking instability, no intermittent claudication, and clear vision. Before collecting medical information, volunteers were asked about their shoe-wear habits and were required to take their socks off for inspection. Name, age, gender, height, weight, blood pressure, and other personal information were included in the questionnaire. In the acquisition test, volunteers performed 10 repetitive tests while walking normally to identify the medial, lateral, midfoot, five metatarsals, thumb, and four toes, dividing the plantar arches artificially into 10 anatomical partitions. Table 1 shows the plantar pressure for different functional area of the foot.

3.2. Point-cloud learning results

The boosting figures for different estimations are plotted in Fig. 6. The difference classifications are c1-c8. According to Fig. 6, there was a boosting with different estimations. c1 has two different zones after boosting, while the remaining seven classifications have

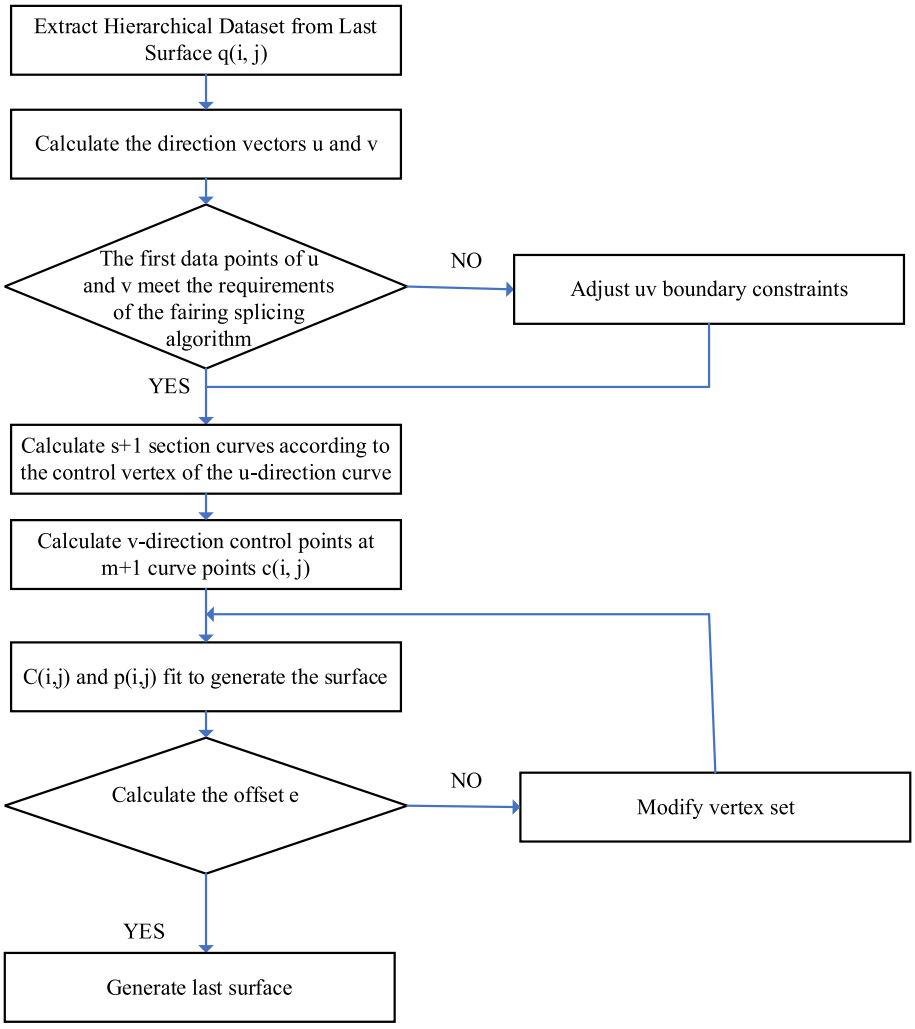

Fig. 5. NURBS surface fitting process based on control points.

three zones. This is the main difference for the different classifications. Here, the x-axis is the pressure value from the plantar pressure dataset, and the y-axis is the number of points. The learning rate for the boosting ensemble learning algorithms was seen in which 30% of the datasets are test sets, and 70% are training datasets. Fig. 7 shows the training-testing percentages (Fig. 7(a)) and ensemble size with accuracies (Fig. 7. (b)); ensemble size means the number of individual base learners or models that are combined to create the final ensemble model. By using different classifiers, the proposed boosting methods are compared for ensemble learning and point cloud classification compared to k nearest neighbor (k-NN), random forest (RF), and naive Bayes (NB) (shown in Fig. 8). The proposed method has higher accuracy (90.8%) than k-NN (87.1%), RF (85.78%), and NB (85.89%).

4. Discussion

4.1. Evaluation using running-in degree

The result is calculated by applying formula (5-7) of the running-in degree in the relevant last design evaluation index in Section 2.2.2. The results of the running-in degree are presented in Table 2, where Control means the control point of NURBS, the value is the pressure value of the point, and fitting is the fitting point. Under the same fitting algorithm proposed in Fig. 5, the data from different sources are averaged for the three running-in degrees, and three types of datasets are applied: preservation morphology, domain segmentation deep learning, and fully convolutional network, as shown in Table 3. In addition, an assessment of the wearing comfort psychological scale can also be performed. Using the Likert scale (1, 3, 5, 7, 9), the scale vocabulary is defined as “very uncomfortable” (1), “discomfort” (3), “moderate” (5), “comfortable” (7), and “very comfortable” (9). The Likert scale is a psychological scale often used in psychological questionnaires. It was developed and named after organizational psychologist Rensis Likert. The self-report

Table 1
Raw dataset of plantar pressure for different zones of the foot using a pressure scan device.

Left	%	N/cm	N/cms	Ns/cm	N/cm
Toe 1	85	5.1	0.02	1.1	0.7
Toe 2-5	25	0.6	0.02	0.1	4.4
Meta 1	85	6.5	0.03	2	0
Meta 2	86	7	0.03	2.2	1.5
Meta 3	86	7.2	0.03	2.4	2.9
Meta 4	84	5	0.16	1.9	2.6
Meta 5	80	1.9	0.06	0.6	0
Midfoot	52	2.9	0.07	0.4	7.3
Heel Medial	55	5.8	1.73	1.1	0
Heel Lateral	53	6.3	1.89	1	6.6
Right	**%**	**N/cm**	**N/cms**	**Ns/cm**	**N/cm**
Toe 1	87	2.6	0.01	0.8	8.1
Toe 2-5	75	0.8	0	0.2	1.5
Meta 1	87	6.6	0.02	2.1	12.8
Meta 2	88	7.9	0.04	2.6	11.7
Meta 3	90	6.1	0.06	2.5	7.7
Meta 4	88	5.1	0.05	1.5	5.1
Meta 5	62	1.4	0.01	0.3	4.4
Midfoot	38	2.3	0.03	0.3	6.2
Heel Medial	41	7.5	0.28	1.2	9.9
Heel Lateral	41	6.3	0.63	1.1	10.6

checklist is one of the most widely used tools in psychological research. On the Likert scale, respondents were asked to rate the comfort level of the product. According to the results of the shoe last optimization design and small batch production, 30 pairs of shoes (five pairs for men and five pairs for women, using three different datasets) were collected from 30 people, and the results of wearing comfort evaluation are shown in Table 4.

Among them, pixel fusion segmentation is the previous research result of the research group; it is mainly through the method of k nearest neighbor (kNN) clustering, and then the image is segmented based on the clustering results. As a result of the evaluation process, we can see that the dataset processed by WUBEL has a low level of running-in (the smaller the value proportional to the error, the more obvious the effect) as well as a higher psychological scale value. Furthermore, the evaluation results exclude the artificial pruning factor of the last body design in the evaluation part of this experiment. From the evaluation process, it can be seen that the dataset processed by WUBEL not only has a low degree of running-in (the smaller the value proportional to the error, the more obvious the effect) but also a higher psychological scale value. In the evaluation part of this experiment, it should be further explained that the evaluation results exclude the artificial pruning factor of the last body design. From the point of view of data generation, last body optimization design and shoe wearing, the last surface optimization guided by dot matrix data based on pressure-sensitive imaging is feasible and effective.

4.2. Applications

4.2.1. Surface design of the last bottom surface based on Delcam

First, the original measurement data of the last female (the data of the last female come from empirical data) are imported; the footprint method is used to form a relatively matching foot corresponding model. Then, the last shoe is repaired and refined by manual experience, and a one-size shoe last is produced, which is usually completed by multiple shoe last designers. After the mother is completed, it is scanned in 3D and imported into the last body design software for meshing operation to provide basic data models for last body trimming, different shoe size expansion and contraction, paired custom processing, and mass production processing. The optimized last design of the basic mother last data is a common design process at present, and the key lies in the collection and processing of the superior last data. Fig. 9 shows an example of the Delcam-based last design process. Among them, Fig. 9 (a) is the visual model of the basic data of the mother last, Fig. 9 (b) is the edge curve and point of the modified shoe last body, and Fig. 9 (b) and Fig. 9 (c) need to fully combine the pressure-sensitive lattice data to continuously optimize the last body correction. Fig. 9 (d) is the trimming process for the last.

4.2.2. Design process of the last bottom surface based on Python-NURBS and easy3D

The pressure-sensing data are organized into a set of lattice data and imported into the Python-NURBS program for surface optimization processing and then imported into the last bottom surface design software for last body design. The general splicing process of the last surface is shown in Fig. 10. Fig. 10 (a) is the different views of the last dataset; Fig. 10(b) id the interface of how the rear rocker of the last body is designed; Fig. 10(c) shows the process of the high waist last design; and Fig. 10 (d) shows the last molding and rendering results.

The last is further trimmed, expanded, and shaped. Finally, these data are imported into the last engraving machine for pre-processing preparation, including knife pattern generation and mass production of the last body, to provide the shoe last entity for the

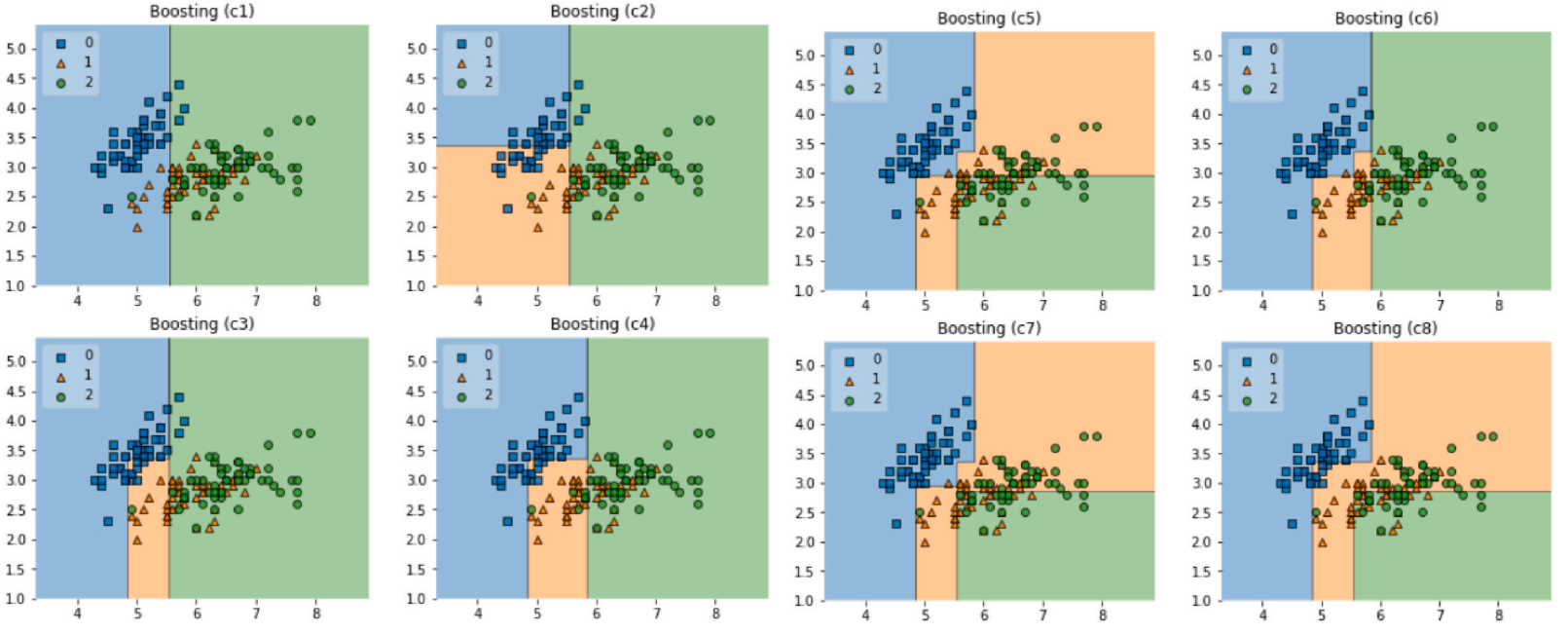

Fig. 6. Different classifications of c1 and c2-c7 for point clouds from the plantar pressure dataset
(a) the performance of the training set and test set (b) the ensemble size of all classification with their accuracy.

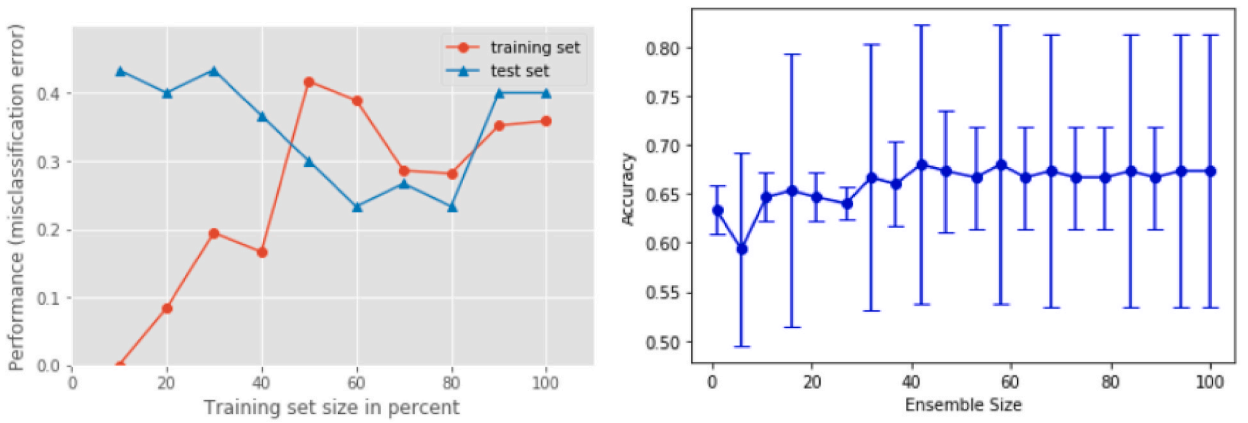

(a) the performance of the training set and test set (b) the ensemble size of all classification with their accuracy

Fig. 7. Training/testing set learning rate (a) and ensemble size accuracy for eight classifications (b).

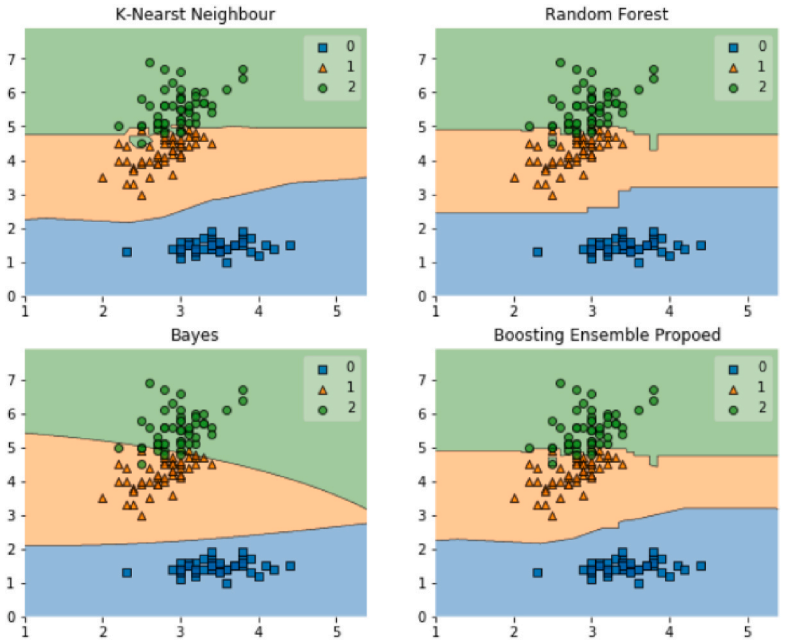

Fig. 8. Comparison of results for different classifiers (a) K-nearest neighbor (b) Random forest (c) Bayes, and (d) Boosting ensemble proposed.

Table 2
Calculation results of point value error and running-in degree (average distance running-in degree).

Order	Control	Value	Fitting Points	Error	Running-in degree
1	(127.877,129.822,158.432)	(127.877,129.822,158.432)	(127.877,129.822,158.432)	−27.322	9.857
2	(89.524,88.965,41.566)	(89.422,147.635,534.522)	(125.236,253.233,24.285)	−17.201	12.530
3	(23.666,24.621,411.321)	(235.211,242.210,146.233)	(100.201,31.254,127.584)	−14.522	5.781
4	(127.356,21.354,101.275)	(124.365,124.358,144.254)	(351.245,301.256,15.222)	−52.231	9.211
5	(125.366,122.235,49.522)	(54.233,57.231,102.233)	(104.253,125.321,58.231)	40.235	5.417
6	(230.212,200.154,18.365)	(12.540,210.231,100.268)	(174.286,152.896,54.396)	27.328	7.697
7	(100.333,105.387,142.65)	(98.632,68.522,107.356)	(170.254,130.256,87.533)	16.957	5.962
8	(201.369,200.365,201.378)	(189.562,175.231,59.63)	(188.564,188.522,73.546)	17.521	7.698
9	(263.365,200.351,198.563)	(201.254,189.524,188.251)	(187.524,156.354,100.587)	21.364	2.752
…	…	…	…	…	…
100	(523.236,400.236,78.365)	(489.521,351.200,140.369)	(488.521,256.321,107.563)	−17.254	11.236

Table 3
The running-in degree calculation of different pressure-sensing algorithm datasets under the same fitting situation.

Methods	Data size	Plantar areas	Average running-in degree
Local Preservation Morphology [22]	100	Front (30), Middle (40), Rear (30)	7.563
Domain Segmentation Deep Learning [23]	102	Front (30), Middle (42), Rear (30)	8.23
Fully Convolutional Network [24]	89	Front (30), Middle (29), Rear (30)	6.588
Pixel fusion segmentation [25]	120	Front (50), Middle (40), Rear (30)	7.544
WUBEL (*)	109	Front (40), Middle (34), Rear (35)	9.874

Table 4
Psychological scale results for different datasets.

Methods	Average scale
Local Preservation Morphology	4.523
Domain Segmentation Deep Learning	6.123
Fully Convolutional Network	6.228
Pixel fusion segmentation	2.567
WUBEL (*)	7.569

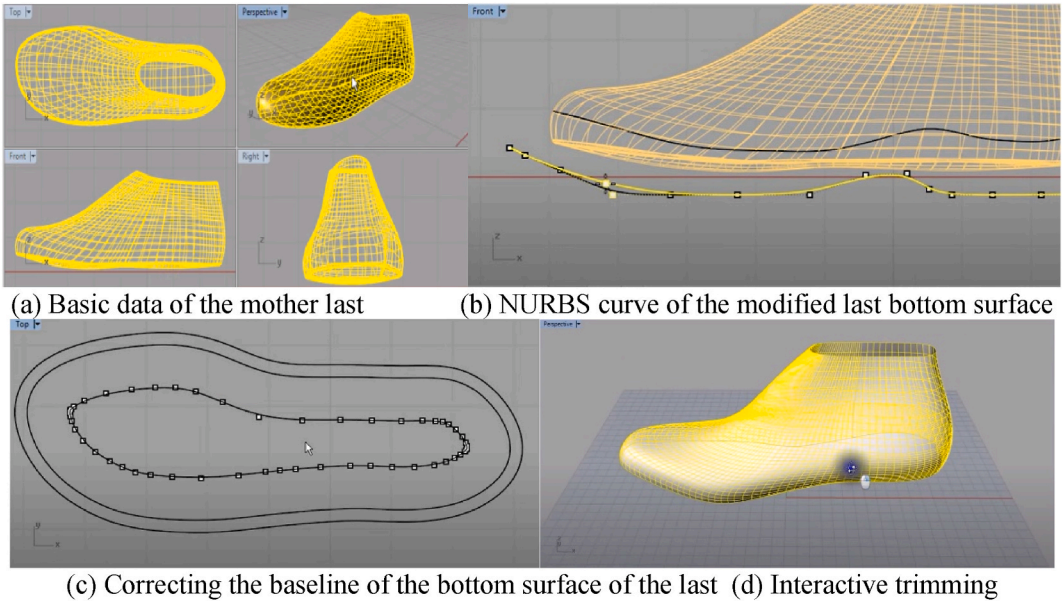

Fig. 9. Delcam's optimization design process based on mother last (a) the basic raw data of the last, (b) NURBS constructed using control points. (c) corrected baseline of the bottom side of the shoe last, and (d) is the interface for interactive trimming process.

subsequent production of comfortable shoes. The interactive last surface optimization design process currently mainly relies on professional shoe last design software. This chapter primarily focuses on whether the dot matrix data generated by the pressure-sensing data can be used for the last design. Through the application of the shoe last comfort design process in this section, it is feasible to use the sensory data for the experimental design study of the superior last design.

5. Conclusions

In this article, the general process of the superior last design from the generation of the NURBS baseline and surface is explained, along with the shoe-last data of the motherboard. The self-defined running-in degree was combined with the psychological scale to evaluate different datasets. The experiment utilizes preservation morphology, domain segmentation deep learning, and fully convolutional network mining technology to study the wearing comfort of finished shoes. Algorithms for ensemble learning are highly accurate. Despite this, the boosting method is a complex training process and is inefficient, which can be improved through algorithm improvements. An approach to improving weak classification algorithms is presented here. Through this method, a prediction function is constructed and then combined in a certain way. Through the operations with the sample set, a sample subset is obtained, and weak classifiers are then generated. The main contributions of this work are to develop a weight-updated boosting-based ensemble learning

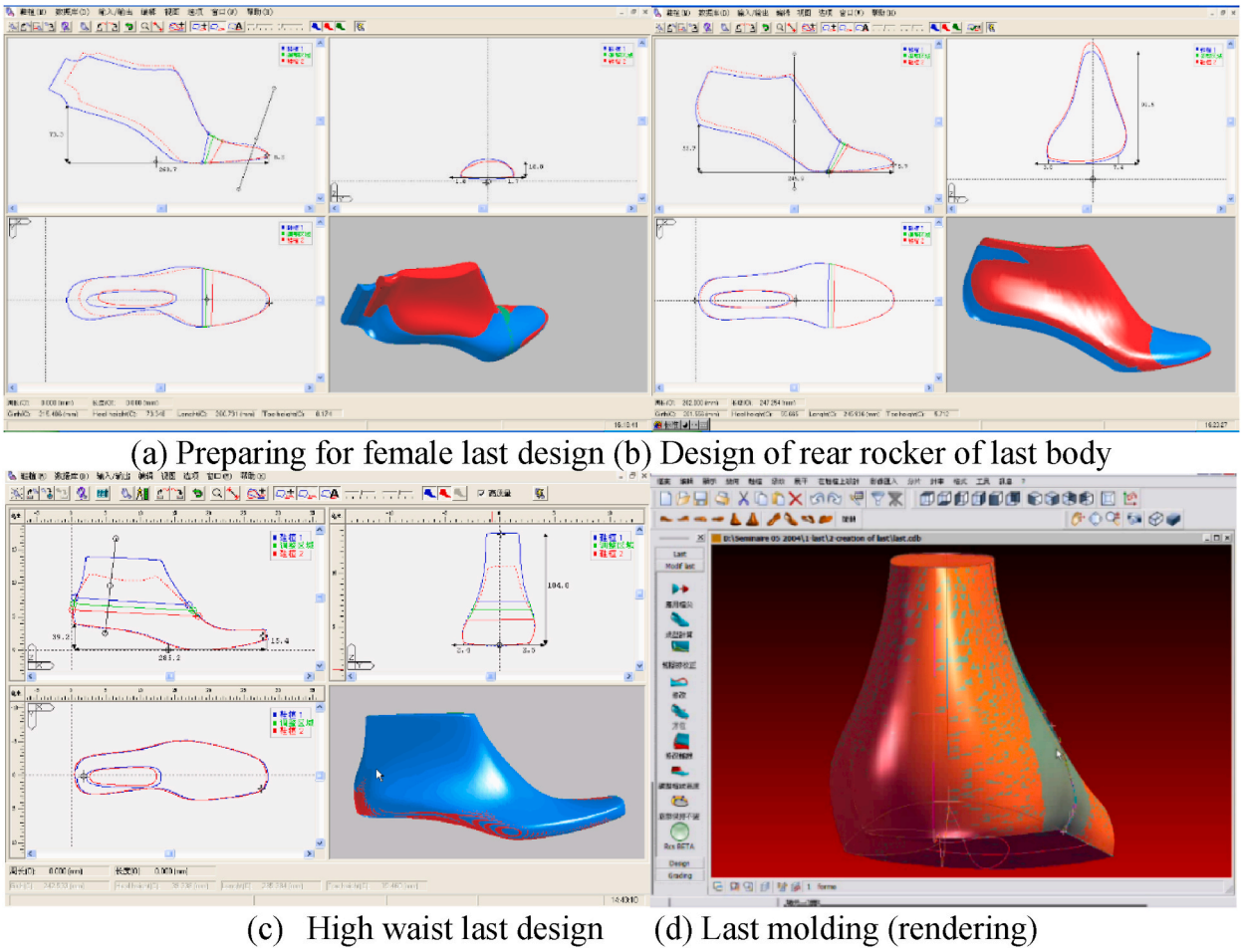

Fig. 10. Shoe last splicing, design, and molding. (a) shoe last in different view, (b) interactive design of the rear rocker last body, (c) high waist last design and (d) rendering result based on the optimization design.

algorithm named WUBEL for generating 3D surfaces based on shoe last point-cloud datasets. This surface will benefit the customization of the shoe-last and improve wearing comfort.

The limitation of the study is the precision of the surface generation. In future works, a feedback system based on real-life tests should be founded. A way to improve shoe last surface generation is to use other NURBS. The shoe's last design should significantly improve the accuracy and efficiency of the process. The NURBS modeling technique has made it possible to create complex, smooth curves and surfaces that accurately replicate the shape of the human foot, resulting in comfortable and well-fitting shoes. However, this area still has room for further research and development. One potential future direction is the integration of machine learning algorithms to automate and optimize the shoe's last design process. Another area of focus could be using advanced materials and manufacturing techniques to enhance the durability and performance of the shoe. Furthermore, it is essential to note that the success of the shoe's last design using NURBS depends heavily on the skill and expertise of the designer. Therefore, future works should also involve the development of training programs and educational resources to train designers on the use of NURBS for shoe last design. On the other hand, the risk of foot injuries in people with diabetes could be effectively mitigated by developing custom shoes based on pressure distribution data from the study results. This is critical in preventing diabetic foot disease and related complications, such as ulcers and infections. By gaining insights into the data on foot pressure distribution from the study results, shoe designers and manufacturers will be able to more accurately design and build shoes for people with diabetes. These shoes can be customized to an individual's foot anatomy and pressure distribution, reducing foot pain, potential ulcers and the risk of diabetic foot disease.

CRediT authorship contribution statement

Dan Wang: Software, Visualization, Writing – original draft. **Zairan Li:** Conceptualization, Supervision, Validation, Writing – review & editing, Funding acquisition. **Nilanjan Dey:** Investigation, Methodology, Resources. **Bitan Misra:** Data curation, Formal analysis. **R. Simon Sherratt:** Methodology, Resources, Supervision. **Fuqian Shi:** Data curation, Investigation, Methodology.

Declaration of competing interest

The authors declare that they have no known competing financial interests or personal relationships that could have appeared to influence the work reported in this paper.

Acknowledgment

This work was supported Wenzhou Science and Technology Bureau Public Science and Technology Project: Personalized Shoe-Last Essence Design Technology for Women's Fashion Shoes under grant no. G20160038.

References

[1] Julian Andres Ramirez-Bautista, Antonio Hernández-Zavala, L. Silvia, Chaparro-Cárdenas, Jorge A. Huerta-Ruelas, Review on plantar data analysis for disease diagnosis, Biocybern. Biomed. Eng. 38 (2) (2018) 342–361, https://doi.org/10.1016/j.bbe.2018.02.004.
[2] Arnaldo G. Leal-Junior, Camilo R. Díaz, Carlos Marques, Maria José Pontes, Frizera Anselmo, 3D-printed POF insole: development and applications of a low-cost, highly customizable device for plantar pressure and ground reaction forces monitoring, Opt Laser. Technol. 116 (2019) 256–264, https://doi.org/10.1016/j.optlastec.2019.03.035.
[3] R.Q. Charles, H. Su, M. Kaichun, L.J. Guibas, PointNet: deep learning on point sets for 3D classification and segmentation, in: Proc. CVPR, Honolulu, HI, USA, 2017, pp. 77–85, https://doi.org/10.1109/CVPR.2017.16.
[4] Y. Guo, H. Wang, Q. Hu, H. Liu, L. Liu, M. Bennamoun, Deep learning for 3D point clouds: a survey, IEEE Trans. Pattern Anal. Mach. Intell. 43 (12) (Dec. 2021) 4338–4364, https://doi.org/10.1109/TPAMI.2020.3005434.
[5] M. Bui, L.-C. Chang, H. Liu, Q. Zhao, G. Chen, Comparative study of 3D point cloud compression methods, in: Proc. BD, Orlando, FL, USA, 2021, pp. 5859–5861, https://doi.org/10.1109/BigData52589.2021.9671822.
[6] P. Zhang, J. Xue, C. Lan, W. Zeng, Z. Gao, N. Zheng, EleAtt-RNN: adding attentiveness to neurons in recurrent neural networks, IEEE Trans. Image Process. 29 (2020) 1061–1073, https://doi.org/10.1109/TIP.2019.2937724.
[7] F. Hu, C. Lin, J. Han, J. Peng, Sementing the Field of Rapeseed from 3D Laser Point Cloud Using Deep Learning, in: Proc AG, Shenzhen, China, 2021, pp. 1–5, https://doi.org/10.1109/Agro-Geoinformatics50104.2021.9530316.
[8] Z. Zhang, J. Sun, Y. Dai, D. Zhou, X. Song, M. He, A representation separation perspective to correspondence-free unsupervised 3-D point cloud registration, Geosci. Rem. Sens. Lett. IEEE 19 (Dec. 2021) 1–5, https://doi.org/10.1109/LGRS.2021.3132926.
[9] S. González, S. García, J.D. Ser, L. Rokach, F. Herrera, A practical tutorial on bagging and boosting based ensembles for machine learning: algorithms, software tools, performance study, practical perspectives and opportunities, Inf. Fusion 64 (2020) 205–237, https://doi.org/10.1016/j.inffus.2020.07.007.
[10] A.S. Khwaja, A. Anpalagan, M. Naeem, B. Venkatesh, Joint bagged-boosted artificial neural networks: using ensemble machine learning to improve short-term electricity load forecasting, Elec. Power Syst. Res. 179 (Feb. 2020), https://doi.org/10.1016/j.epsr.2019.106080.
[11] W. Lu, Z. Li, J. Chu, Adaptive ensemble undersampling-boost: a novel learning framework for imbalanced data, J. Syst. Software 132 (Oct. 2017) 272–282, https://doi.org/10.1016/j.jss.2017.07.006.
[12] S.S. Nath, G. Mishra, J. Kar, S. Chakraborty, N. Dey, A survey of image classification methods and techniques, in: Proc. ICCICCT, Kanyakumari, India, 2014, pp. 554–557, https://doi.org/10.1109/ICCICCT.2014.6993023.
[13] B. Cheng, W. Wu, D. Tao, S. Mei, T. Mao, J. Cheng, Random cropping ensemble neural network for image classification in a robotic arm grasping system, IEEE Trans. Instrum. Meas. 69 (9) (Sept. 2020) 6795–6806, https://doi.org/10.1109/TIM.2020.2976420.
[14] Y. Zhang, G. Cao, X. Li, Multiview-based random rotation ensemble pruning for hyperspectral image classification, IEEE Trans. Instrum. Meas. 70 (Jul. 2021) 1–14, https://doi.org/10.1109/TIM.2020.3011777.
[15] L. Ma, X. Wu, Z. Li, High-precision medicine bottles vision online inspection system and classification based on multifeatures and ensemble learning via independence test, IEEE Trans. Instrum. Meas. 70 (Oct. 2021) 1–12, https://doi.org/10.1109/TIM.2021.3121465.
[16] B. Dong, Z. Huang, Y. Guo, Q. Wang, Z. Niu, W. Zuo, Boosting weakly supervised object detection by learning bounding box adjusters, in: Proc ICCV, Montreal, QC, Canada, 2021, pp. 2856–2865, https://doi.org/10.1109/ICCV48922.2021.00287.
[17] H. Cao, S. Bernard, R. Sabourin, L. Heutte, Random forest dissimilarity based multiview learning for radiomics application, Pattern Recogn. 88 (Apr. 2019) 185–197, https://doi.org/10.1016/j.patcog.2018.11.011.
[18] S.F. Stefenon, R. Bruns, A. Sartori, L.H. Meyer, R.G. Ovejero, V.R.Q. Leithardt, Analysis of the ultrasonic signal in polymeric contaminated insulators through ensemble learning methods, IEEE Access 10 (Mar. 2022) 33980–33991, https://doi.org/10.1109/ACCESS.2022.3161506.
[19] A.L. Kleppe, L. Tingelstad, O. Egeland, Coarse alignment for model fitting of point clouds using a curvature-based descriptor, IEEE Trans. Autom. Sci. Eng. 16 (2) (Apr. 2019) 811–824, https://doi.org/10.1109/TASE.2018.2861618.
[20] K. Sharma, J. Virmani, A decision support system for classification of normal and medical renal disease using ultrasound images: a decision support system for medical renal diseases, Int. J. Ambient Comput. Intell. (IJACI) 8 (2) (2017) 52–69, https://doi.org/10.4018/IJACI.2017040104.
[21] M.N.Y. Ali, M.G. Sarowar, M.L. Rahman, J. Chaki, N. Dey, J.M.R. Tavares, Adam deep learning with SOM for human sentiment classification, Int. J. Ambient Comput. Intell. (IJACI) 10 (3) (2019) 92–116, https://doi.org/10.4018/IJACI.2019070106.
[22] Z. Tian, N. Dey, A.S. Ashour, et al., Morphological segmenting and neighborhood pixel-based locality preserving projection on brain fMRI dataset for semantic feature extraction: an affective computing study, Neural Comput. Appl. 30 (2018) 3733–3748, https://doi.org/10.1007/s00521-017-2955-2.
[23] Daniel Franco-Barranco, Julio Pastor-Tronch, Aitor González-Marfil, Ignacio Arrate Muñoz-Barrutia, Arganda-Carreras, Deep learning based domain adaptation for mitochondria segmentation on EM volumes, Comput. Methods Progr. Biomed. 222 (2022) 106949, https://doi.org/10.1016/j.cmpb.2022.106949.
[24] NimaSadeghzadeh NacerFarajzadeh, Mahdi Hashemzadeh, A fully convolutional residual encoder-decoder neural network to localize breast cancer on histopathology images, Comput. Biol. Med. 147 (2022) 105698, https://doi.org/10.1016/j.compbiomed.2022.105698.
[25] S. Wang, Y. Zhao, A novel patch-based multi-exposure image fusion using super-pixel segmentation, IEEE Access 8 (Feb. 2020) 39034–39045, https://doi.org/10.1109/ACCESS.2020.2975896.

Dan Wang received a Ph.D. degree from Tianjin Key Laboratory of Process Measurement and Control, School of Electrical Engineering and Automation, Tianjin University. She is now an Assistant Professor at Wenzhou Polytechnic. Dr. Wang has published over 20 papers and conference proceedings; her research interests include optical pressure measurement, data analysis and image processing.

Zairan Li received his Ph.D. degree from Tianjin Key Laboratory of Process Measurement and Control, School of Electrical Engineering and Automation, Tianjin University. Dr. Li is now a Full Professor at Wenzhou Polytechnic. Dr. Li has published over 40 papers and conference proceedings; his research interests include fuzzy logic, image mining, industrial design, intelligent design machine learning, biomedical imaging technologies and artificial intelligence in industrial applications.

Nilanjan Dey (Senior Member, IEEE) received his B.Tech. degree in Information Technology from the West Bengal University of Technology in 2005, M. Tech. in Information Technology in 2011 from the same university and a Ph.D. in digital image processing in 2015 from Jadavpur University, India. In 2011, he was appointed as an Assistant Professor in the Department of Information Technology at JIS College of Engineering, Kalyani, India, followed by Bengal College of Engineering College, Durgapur, India, in 2014. He is now employed as an Associate Professor in the Department of Computer Science and Engineering, Techno International New Town, Kolkata, India. His research topics are signal processing, machine learning, and information security. Dr. Dey is an Associate Editor of IET Image Processing and is currently the Editor-in-Chief of the International Journal of Ambient Computing and Intelligence (IJACI) and Series Coeditor of Springer Tracts of Nature-Inspired Computing (STNIC).

Bitan Misra received her B.tech and M.tech dual degree in Electronics and Telecommunication Engineering from KIIT University, Bhubaneswar, India in 2018. She received her Ph.D. in 2022 from the National Institute of Technology, Durgapur, India. Her main research interests include optimization techniques, deep learning, evolutionary algorithms and soft computing techniques.

R. Simon Sherratt (Fellow, IEEE) received a B.Eng. from Sheffield City Polytechnic in 1992, M.Sc. from The University of Salford in 1993, and Ph.D. from The University of Salford in 1996. In 1996, he was appointed as a Lecturer in Electronic Engineering with the University of Reading, where he is currently a Professor of Biosensors. His research area is wearable devices, mainly for healthcare and emotion detection. Eur Ing Professor Sherratt was awarded the 1st place IEEE Chester Sall Award in 2004, 2nd place in 2014, 3rd place in 2015 and 3rd place in 2016 for best papers in the IEEE Transactions on Consumer Electronics.

Fuqian Shi (Senior Member, IEEE) graduated from the College of Computer Science and Technology, Zhejiang University, received his Ph.D. in Engineering and was a visiting Associate Professor at the Department of Industrial Engineering and Management Systems, University of Central Florida, USA from 2012 to 2014. He is a Senior Member of IEEE, Membership of ACM; and serves as over 50 committee board members of international conferences; Dr. Shi also serves as an Associate Editor of the International Journal of Ambient Computing and Intelligence (IJACI), International Journal of Rough Sets, and Data Analysis (IJRSDA). Dr. Fuqian has published over 120 journal papers and conference proceedings; his research interests include fuzzy inference systems, artificial neural networks, biomechanical engineering, and bioinformatics.